HHS Public Access

Author manuscript

Invest Radiol. Author manuscript; available in PMC 2019 May 01.

Published in final edited form as:

Invest Radiol. 2018 May ; 53(5): 257–263. doi:10.1097/RLI.0000000000000434.

Relaxivity of ferumoxytol at 1.5T and 3.0T

Gesine Knobloch, MD[*1], **Timothy Colgan, PhD**[*1,2], **Curtis N Wiens, PhD**[*1], **Xiaoke Wang**[*1,3], **Tilman Schubert, MD**[*1], **Diego Hernando, PhD**[*2], **Samir D Sharma, PhD**[*1], and **Scott Reeder, MD, PhD**[*1,2,3,4,5]

[*1] Department of Radiology, University of Wisconsin – School of Medicine and Public Health, Madison, WI, USA

[*2] Department of Medical Physics, University of Wisconsin – School of Medicine and Public Health, Madison, WI, USA

[*3] Department of Biomedical Engineering, University of Wisconsin – School of Medicine and Public Health, Madison, WI, USA

[*4] Department of Medicine, University of Wisconsin – School of Medicine and Public Health, Madison, WI, USA

[*5] Department of Emergency Medicine, University of Wisconsin – School of Medicine and Public Health, Madison, WI, USA

Abstract

Objectives—To determine the relaxation properties of ferumoxytol, an off-label alternative to gadolinium based contrast agents (GBCA), under physiological conditions at 1.5T and 3.0T.

Materials and Methods—Ferumoxytol was diluted in gradually increasing concentrations (0.26–4.2 mM) in saline, human plasma and human whole blood. MR relaxometry was performed at 37˚C at 1.5T and 3.0T. Longitudinal and transverse relaxation rate constants (R1, R2, R2*) were measured as a function of ferumoxytol concentration and relaxivities (r1, r2, r2*) were calculated.

Results—A linear dependence of R1, R2 and R2* on ferumoxytol concentration was found in saline and plasma with lower R1 values at 3.0T and similar R2 and R2* values at 1.5T and 3.0T (1.5T: $r1_{saline}$ = 19.9 ± 2.3 $s^{-1}mM^{-1}$, $r1_{plasma}$ = 19.0 ± 1.7 $s^{-1}mM^{-1}$; $r2_{saline}$ = 60.8 ± 3.8 $s^{-1}mM^{-1}$; $r2_{plasma}$ = 64.9 ± 2.3 $s^{-1}mM^{-1}$; $r2^*_{saline}$ = 60.4 ± 1.3 $s^{-1}mM^{-1}$; $r2^*_{plasma}$ = 64.4 ± 0.3 $s^{-1}mM^{-1}$; 3.0T: $r1_{saline}$ = 10.0 ± 0.3 $s^{-1}mM^{-1}$, $r1_{plasma}$ = 9.5 ± 0.2 $s^{-1}mM^{-1}$; $r2_{saline}$ = 62.3 ± 3.7 $s^{-1}mM^{-1}$; $r2_{plasma}$ = 65.2 ± 1.8 $s^{-1}mM^{-1}$; $r2^*_{saline}$ = 57.0 ± 3.6 $s^{-1}mM^{-1}$; $r2^*_{plasma}$ = 55.7 ± 4.4 $s^{-1}mM^{-1}$). The dependence of relaxation rates on concentration in blood was nonlinear. Formulas from 2nd order polynomial fittings of the relaxation rates were calculated to characterize the relationship between $R1_{blood}$ and $R2_{blood}$ with ferumoxytol.

Conclusions—Ferumoxytol demonstrates strong longitudinal and transverse relaxivities. Awareness of the nonlinear relaxation behavior of ferumoxytol in blood is important for ferumoxytol-enhanced MRI applications and for protocol optimization.

Corresponding Author: Gesine Knobloch, MD, Department of Radiology, University of Wisconsin – School of Medicine and Public Health, Wisconsin Institute of Medical Research (WIMR-2), 1111 Highland Avenue, Madison, WI, 53705, USA, gknobloch@wisc.edu, Phone: +1-608-265-6011,Fax: +1-608-265-6011.

Keywords

contrast media; ferumoxytol; superparamagnetic iron oxide; relaxometry; relaxation rate constant; relaxivity; magnetic resonance imaging

Introduction

Ferumoxytol (Feraheme, AMAG, Waltham, MA, USA) is an ultra-small superparamagnetic iron oxide (USPIO) approved by the US Food and Drug Administration (FDA) for intravenous treatment of iron deficiency anemia in adults with chronic kidney disease (1, 2). It can be used off-label as a contrast agent (CA) for magnetic resonance imaging (MRI) and has drawn increasing interest for this application due to growing concerns regarding the safety of gadolinium based contrast agents (GBCAs) (3).

In addition to the association between ACR class one GBCA exposure and the occurrence of nephrogenic systemic fibrosis (NSF) in patients with impaired renal function, the phenomenon of gadolinium deposition in the brain has been described more recently. Although the clinical significance of gadolinium deposition is unknown, concerns regarding the potential risks of this phenomenon have been raised. These concerns have led to divergent precautionary recommendations between different regulatory bodies and radiological societies (4–8) and foster the search for alternative contrast agents. Since iron is a physiologically necessary element for normal metabolism, ferumoxytol may be a promising alternative to GBCA.

The physiochemical and pharmacokinetic properties of ferumoxytol, including its long intravascular half-life of 10–14 hours and high relaxivity without protein binding, are useful for a variety of emerging clinical and preclinical MRI applications, such as arterial phase and steady state phase cardiovascular imaging (9–13), imaging of inflammation (14–16) and, based on its excretion via the reticuloendothelial system (RES), imaging of the liver, bone marrow, spleen and lymph nodes (13, 17–20). Optimization of imaging and dosing protocols of ferumoxytol enhanced MRI and MR-angiography (MRA) requires precise characterization of its MR relaxation properties. Further, quantitative applications that aim to measure the tissue concentration of ferumoxytol require precise knowledge of the MR relaxation properties. Although several studies have reported relaxation rates of ferumoxytol at 0.47 Tesla (T) and 1.5T (10–12, 21), these data are mostly limited to the bare mentioning of values without providing a systematic investigation of relaxivities over a wide range of ferumoxytol concentrations under physiological conditions. No data are available for 3.0T.

The magnetic relaxation properties of the water proton (^{1}H) signal in the presence of contrast agents are highly dependent on the physiological environment and the effects of water/^{1}H compartmentalization (22, 23). In addition, MR relaxivity in the presence of superparamagnetic iron oxide nanoparticles is highly dependent on the particles' spatial biodistribution (21) and therefore need to be taken into special consideration. Furthermore, several other factors influence ^{1}H relaxivity, such as direct dipolar interactions, motion due to blood flow or cells within fluid, the level of tissue oxygenation, protein binding of the

reagent, temperature, and magnetic field strength. It is therefore essential to measure relaxivity under (near-) physiological conditions and at relevant magnetic field strengths.

For these reasons, the purpose of this in vitro study was to determine the relaxivity characteristics of ferumoxytol at physiological temperatures in saline, human plasma and human whole blood at clinically relevant field strengths (1.5T and 3.0T).

Materials and Methods

An exemption was obtained from the local institutional review board (IRB) to conduct this in vitro study.

Sample Preparation

To account for any biological variability, a total of six units of fresh (no older than 42 days) human packed red blood cells (RBC) and 12 compatible units of human plasma were obtained from the local blood bank. Six units of plasma were combined to obtain an averaged plasma sample. The residual six units of plasma where mixed with the six units of compatible RBC to reconstitute whole blood.

Ferumoxytol was diluted in 30 mL sample tubes of saline (n=5), human plasma (n=5) and human whole blood (n=5) at five gradually increasing concentrations within the range typically used in clinical imaging (1/2048 [0.26 mM], 1/1024 [0.52 mM], 1/512 [1.05 mM], 1/256 [2.1 mM], 1/128 [4.2 mM]). The 15 sample tubes were sealed and then placed in an MR compatible water bath at 37°C for 20 minutes before imaging in the MR-scanner. To avoid settling of particles or cells, samples were inverted gently every 15–20 minutes.

Circulating water bath

An MR compatible temperature controlled water bath was constructed (setup Figure 1): A 900 W water-revolving heater (Anova Precision Cooker, Anova Culinary, San Francisco, CA; accuracy ±0.01°C), with the temperature control set to 37°C, and a 10 L water container were placed in the MR-control room (Zone 3). A roller pump (S3 Roller Pump, Stockert Instrumente GmbH, Munich, Germany) in the control room was used to pump the heated water via two vinyl tubes through the waveguide in and back out of a second 10 L water container inside the MR-scanner. This second water container contained our sample tubes. An MR compatible thermometer (ReFlex Signal Conditioner, Neoptix, Canada; accuracy ±0.8°C) in the control room was used to monitor the actual water temperature of the phantom-containing second water container inside the MR-scanner via a fiberoptic probe.

For measurements of the longitudinal (R1=1/T1) and transverse relaxation rate constants (R2=1/T2), the water bath was doped with 10 mM of manganese chloride. This reduced the long T1 and T2 of water and helped reduce motion artifacts due to the flowing water. A different water bath was used for the R2* (R2*=1/T2*) measurements, which was doped with 1 mM of copper sulfate. This reduced the long T1 of the water bath while maintaining a longer T2* so the gradient echo signal did not decay rapidly.

Measurements of Relaxivity Curves

Relaxivity measurements were made on a 1.5T clinical MRI system (Signa HDxt, GE Healthcare, Waukesha, WI) using an 8-channel phased array torso coil (USA Instruments, Cleveland, OH) and a 3.0T MRI system (Discovery MR 750, GE Healthcare, Waukesha, WI) using a 32-channel phased array torso coil (Neocoil, Pewaukee, WI). Acquisition parameters for R1, R2 and R2* measurements are summarized in Table 1. No parallel imaging was applied at any time. R1, R2 and R2* maps were generated in MATLAB (MathWorks, Natick, MA).

R1 measurements

R1 measurements were made using a coronal 2D fast spin echo inversion recovery sequence with multiple (n=10) logarithmically spaced inversion times that were chosen to cover the range of our expected R1 values (Table 1). R1 maps were generated using a nonlinear least squares fitting algorithm in MATLAB (trust region reflective algorithm).

R2 measurements

R2 measurements were made with multiple echoes from a coronal 2D spin echo sequence (Table 1). R2 maps for each vial were generated using a nonlinear least squares fitting algorithm in MATLAB (graph cut algorithm (24)) from the magnitude data of the multiple spin echo images. Only the echoes where the signal was significantly above the noise floor were used in the fitting procedure, which was determined manually for each vial using the time history of several points for each vial and approximating a value for the noise floor.

R2* measurements

R2* measurements from a free induction decay were done with an investigational version of a coronal 3D multiecho spoiled gradient echo (SGRE) chemical shift-encoded (CSE) method (IDEAL-IQ, GE Healthcare, Waukesha, WI). Axial reconstructions of these 3D acquisitions also served as a visual control for all T1 and T2 measurements to check that no settling of particles (ferumoxytol, RBC, and/or protein), as seen by spatial gradients of R2* in the vertical direction within the vials, has occurred.

Two separate 3D SGRE measurements were used to measure R2* values, one with a short initial TE to measure the three highest concentration of ferumoxytol vials (1.05–4.2 mM) and one with a longer initial TE to measure the remaining two low concentration vials (0.26–0.52 mM) (Table 1). At 1.5T, both acquisitions consisted of a single echo train with monopolar readout. At 3.0T, both acquisitions consisted of two interleaved echo trains with a monopolar readout. R2* maps were reconstructed in MATLAB using a nonlinear least-squares fitting of the complex-valued multiecho images (24).

Calculation of Relaxivities and Statistical Analyses

For calculation of the relaxation rate constants, R1, R2 and R2* maps were loaded into MATLAB. A 1.5 cm^2 circular region of interest (ROI) was positioned centrally within each vial of the 18 sample tubes and then copied and pasted to three equally distanced slices to ensure perfect co-registration between the measurements. Slices were chosen to cover an

upper, middle and lower section of the sample tubes to account for possible minor differences in relaxation rates that might have occurred due to setting of particles, despite repeated inversion of the vials. Mean R1, R2 and R2* values and standard deviations (STD) were collected in a spreadsheet (Microsoft Excel 2016) and then averaged between the three slices. Data were examined visually in scatterplots. For all ferumoxytol in saline and plasma dilutions, linear regression of R1, R2 and R2* values and ferumoxytol concentration was used to determine r1, r2, and r2* based on the slope of the regression. Linear regression fit of ferumoxytol in blood was poor. Therefore, 2nd order polynomial regression of R1, R2 and R2* values and ferumoxytol concentration was performed for the ferumoxytol in blood dilutions. Standard errors (SE) of the fits for r1, r2, and r2* were calculated in SPSS (IPSS Inc., version 23.0, IBM, Chicago, IL).

Results

Calculated mean relaxivity values and standard errors of all measurements are summarized in Table 2. Table 3 summarizes the regression formulas that determined the experimentally measured relaxivities (r1, r2 and r2*) in saline, plasma and blood at 1.5T and 3.0T.

No relevant settling of particles or red blood cells was observed, either visually in the 3D multiecho SGRE sequence, or quantitatively in the ROI measurements that were conducted in the three slices of each vial.

r1 relaxivities

Figure 2A shows the r1 relaxivity curves of ferumoxytol in saline, plasma, and blood.

The dependences of saline and plasma on ferumoxytol concentrations were highly linear, as evidenced visually and by the high correlation coefficients (Table 3). We note that the R1 values at 1.5T (saline: 19.9 ± 2.3 $s^{-1}mM^{-1}$, plasma: 19.0 ± 1.7 $s^{-1}mM^{-1}$) were almost exactly twice that at 3.0T (saline: 10.0 ± 0.3 $s^{-1}mM^{-1}$, plasma: 9.5 ± 0.2 $s^{-1}mM^{-1}$).

R1 relaxivity in blood had very nonlinear behavior. After an initial linear course that resembled the behavior in saline and plasma at lower ferumoxytol concentrations, the relaxivity curve departed into a plateau at higher ferumoxytol concentrations above 2.1 mM. Fitting of ferumoxytol concentration in blood was excellent using the 2nd order polynomial regression (Table 3). At 1.5T, we observed high standard deviations of the R1 measurement for saline, plasma and blood vials with the highest ferumoxytol concentration (4.2 mM) due to the extreme shortening of the transverse relaxation time, T2, which led to low signal to noise (SNR) and noisy R1 maps (Table 2; Figure 2A).

r2 relaxivities

Figure 2B shows the r2 relaxivity curves of ferumoxytol in saline, plasma, and blood. As with R1, the dependences of R2 in saline and plasma on ferumoxytol concentrations were highly linear, as evidenced by the high correlation coefficients (Table 3). R2 values for saline and plasma were similar (1.5T saline: 60.8 ± 3.8 $s^{-1}mM^{-1}$, plasma: 64.9 ± 1.8 $s^{-1}mM^{-1}$; 3.0T saline: 62.3 ± 3.7 $s^{-1}mM^{-1}$, plasma: 65.2 ± 1.8 $s^{-1}mM^{-1}$; Figure 2).

R2 relaxivity in blood, however, was nonlinear with an initial steeper slope at lower ferumoxytol concentrations that subsequently flattened at concentrations greater than 2.1 mM, with a slope similar to the one of saline and plasma. Fitting of ferumoxytol concentration in blood was excellent with a 2nd order polynomial regression (Table 3). R2 relaxivities were about the same between 1.5T and 3.0T for all three media, saline, plasma, and blood (slope of 1 when plotting R2 values at 1.5T against values at 3.0T), indicating an independence of R2 from the field strength (Figure 3A).

r2* relaxivities

Figure 2C shows the r2* relaxivity curves of ferumoxytol in saline, plasma, and blood. Again, the dependences of saline and plasma on ferumoxytol concentrations were highly linear, as evidenced by the high correlation coefficients (Table 3). R2* values of saline and plasma at 1.5T (saline: 60.4 ± 4.7 $s^{-1}mM^{-1}$; plasma: 64.4 ± 2.5 $s^{-1}mM^{-1}$) and 3.0T (saline: 57.0 ± 4.7 $s^{-1}mM^{-1}$; plasma: 55.7 ± 4.4 $s^{-1}mM^{-1}$) were similar to the corresponding R2 values (slope of 0.9–1.0 when plotting R2 against R2* values at 1.5T and 3.0T), indicating little to no refocusable transverse magnetization in saline and plasma (Figure 3B).

The R2* relaxivity in blood, however, like R2, was nonlinear with progressively higher R2* values with increasing ferumoxytol concentrations that did not plateau. Fitting of R2* in blood with ferumoxytol was excellent with a 2nd order polynomial regression (Table 3). Relaxivities were very similar between 1.5T and 3.0T for all three media, saline, plasma, and blood (slope of 0.9–1.0 when plotting R2* values at 1.5T against values at 3.0T), indicating that R2* of these ferumoxytol solutions is independent of field strength (Figure 3C).

Discussion

This study measured the relaxivity characteristics of ferumoxytol in saline, human plasma and human whole blood at near physiological conditions (37°C) and at 1.5T and 3.0T. r1, r2 and r2* relaxivities of saline and plasma were highly linear, whereas the relaxivity of ferumoxytol in blood was more complex and nonlinear.

The longitudinal and transverse relaxivities of saline and of plasma were almost identical. This was largely anticipated since ferumoxytol has no known protein binding in plasma that would slow the rate of molecular tumbling and thereby increase the spin interactions between ferumoxytol and the surrounding water protons (23).

This study also demonstrated that R1 values of ferumoxytol in saline and plasma were twice as high at 1.5T compared to 3.0T, consistent with previous studies showing generally higher longitudinal relaxivity at lower field strengths (21, 25, 26). Furthermore, we demonstrated that R2 values in saline and plasma were almost equal to the transverse relaxation rate constants from free induction decay (R2*). This result was also anticipated because only stationary spins that experience a constant magnetic field within the tissue can be fully refocused as part of the spin echo acquisition. In saline and plasma however, the water protons are in constant motion due to diffusion and experience an alternating magnetic field from the inhomogeneities caused by the contrast agent. For this reason, in saline and plasma,

spins elude effective refocusing by the spin echo sequence. Lastly, R2 and R2* measured in saline and plasma with ferumoxytol showed similar results at 1.5T and 3.0T. This can be explained by the superparamagnetic properties of ferumoxytol, which is an SPIO that saturates at its maximum induced magnetization at much lower field strengths (0.25T) and is therefore already fully saturated at both, 1.5T and 3.0T (27).

In contrast to homogeneous solutions like saline or plasma, R1, R2, and R2* relaxation rate constants of blood with increasing ferumoxytol concentrations showed a nonlinear behavior with increases in ferumoxytol concentration. We speculate that this may be due in part to two separate effects:

First, compartmentalization of water in blood can occur with increasing contrast agent concentrations. It was found that increasing CA concentration results in decreased cell membrane permeability and active (oxygen and ATP-dependent) ^{1}H exchange between the intra- and extracellular space (23, 28). The gradually increasing compartmentalization of extracellular spins that are directly-interacting with the contrast agent and intracellular spins that do not directly interact with the contrast agent leads to the development of magnetic gradients with vastly different relaxation rate constants between the intracellular and extracellular spaces (23, 28). In our study, the water compartmentalization effect in blood on longitudinal relaxivity seems to set in at ferumoxytol concentrations greater than 2.1 mM when R1 values depart from linear behavior when the slower intracellular longitudinal relaxivity rate becomes more pronounced. Likewise, with beginning of the ^{1}H compartmentalization, the progressively intracellular trapped spins now experience a stable and homogeneous magnetic field, which can be refocused by the 180 degree pulse of a spin-echo sequence and might explain the flattening of the R2 curve in blood at higher ferumoxytol concentrations (≥2.1 mM).

Second, the spatial distribution or aggregation of ferumoxytol strongly affects the transverse relaxation of superparamagnetic particles (21). In blood, ferumoxytol is restricted to the extracellular place (plasma: ~55–60 % of the total blood volume). The relative aggregation of ferumoxytol within a smaller volume leads to microscopically heterogeneous magnetization within the voxels, which leads to a markedly increased dephasing of spins compared to saline or plasma where ferumoxytol is distributed uniformly throughout each voxel. This effect likely explains the steeper r2 and r2* slope of ferumoxytol in blood.

The measured blood r1 relaxivity values in our study are in good agreement with previous results (11, 21) that reported values between 12–15 $s^{-1}mM^{-1}$ at 1.5T and 37°C with ferumoxytol concentrations of about 4 mg Fe/kg. This corresponds to a normal dose of approximately 0.07 mmol/kg or an approximate steady-state blood concentration of ~1.16 mM in an average 75 kg person with a blood volume of 4.5 liters. Recent ex-vivo studies however suggest, that the dose of ferumoxytol that optimizes the signal to noise in steady state is 2.5 mM (~8.4 mg/kg) (9). For a 75 kg person, this dose is 630 mg, exceeding a single bottle (510 mg, or approximately 2.0 mM (6.8 mg/kg) for a 75 kg person) which has important cost implications. It should also be noted that the U.S. and European regulatory authorities have issued strong safety warnings about severe allergic reactions after the administration of ferumoxytol. These warnings led to the withdrawal of ferumoxytol from

the European market in 2015 and warnings from the FDA in 2015 (29–31). Previously reported r2 relaxivity for ferumoxytol at 1.5T was 89 s-1mM-1 (21), higher than measured in our study. However, the details of how and in which media these relaxivity values were measured previously was not reported. To the best of or our knowledge, no relaxivity values of ferumoxytol have ever been reported for 3.0T.

This study has several limitations. First, due to the nature of this in vitro study, alterations in relaxivity due to blood flow or other factors related to the preparation could not be taken into consideration. Second, our measurements were conducted in at least partly deoxygenated venous blood. This may have affected apparent relaxation rates by altering the transmembrane water exchange in erythrocytes and the concentration of paramagnetic deoxygenated hemoglobin. However, we expect the overall impact of these effects to be very small. Future studies investigating the relaxivities of ferumoxytol in oxygenated blood may be helpful to determine the true magnitude of these effects, if any. Finally, the hematocrit may have influenced the relaxivity and MR characteristics of ferumoxytol. We attempted to mitigate the effects of biological variability of hematocrit by mixing the blood and plasma units from 6 adult donors to generate average physiological values with a hematocrit of about 40–45% and hemoglobin of about 12–13 g/dl.

In conclusion, the ferumoxytol relaxivity values reported in this study may serve as the basis for future dosing and protocol optimization strategies for the off-label use of this substance as an MR-contrast agent at 1.5T and 3.0T. Further, these results provide the basis for quantitative ferumoxytol enhanced MRI methods that require underlying knowledge of the MR relaxivity properties of this agent.

Acknowledgments

Sources of Funding:

This project received R&D grant support by the Departments of Radiology and Medical Physics, University of Wisconsin, as well as the NIH (K24 DK102595). Furthermore, the authors wish to acknowledge support from GE Healthcare and Bracco Diagnostics who provide research support to the University of Wisconsin.

References

1. Lu M, Cohen MH, Rieves D, Pazdur R. FDA report: Ferumoxytol for intravenous iron therapy in adult patients with chronic kidney disease. Am J Hematol. 2010;85(5):315–9. [PubMed: 20201089]
2. Spinowitz BS, Kausz AT, Baptista J, et al. Ferumoxytol for treating iron deficiency anemia in CKD. J Am Soc Nephrol. 2008;19(8):1599–605. [PubMed: 18525001]
3. Fraum TJ, Ludwig DR, Bashir MR, Fowler KJ. Gadolinium-based contrast agents: A comprehensive risk assessment. J Magn Reson Imaging. 2017;46(2):338–53. [PubMed: 28083913]
4. PRAC 2017;Pages. Accessed at http://www.ema.europa.eu/docs/en_GB/document_library/Press_release/2017/03/WC500223209.pdf Accessed March 10, 2017.
5. ACR 2017;Pages. Accessed at https://www.acr.org/About-Us/Media-Center/Press-Releases/2017-Press-Releases/20170404-ACR-Response-to-the-European-PRAC-Recommendations. Accessed July 22, 2017 2017.
6. Gulani V, Calamante F, Shellock FG, et al. Gadolinium deposition in the brain: summary of evidence and recommendations. The Lancet Neurology. 2017;16(7):564–70. [PubMed: 28653648]
7. FDA 2017;Pages. Accessed at https://www.fda.gov/Drugs/DrugSafety/ucm455386.htm. Accessed July 25, 2017.

8. FDA 2017;Pages. Accessed at https://www.fda.gov/Safety/MedWatch/SafetyInformation/SafetyAlertsforHumanMedicalProducts/ucm559709.htm. Accessed July 25, 2017.
9. Reeder SB, Smith MR, Hernando D. Mathematical optimization of contrast concentration for t1-weighted spoiled gradient echo imaging. Magnetic Resonance in Medicine. 2016;75(4):1556–64. [PubMed: 25981460]
10. Finn JP, Nguyen KL, Han F, et al. Cardiovascular MRI with ferumoxytol. Clin Radiol. 2016;71(8): 796–806. [PubMed: 27221526]
11. Prince MR, Zhang HL, Chabra SG, et al. A pilot investigation of new superparamagnetic iron oxide (ferumoxytol) as a contrast agent for cardiovascular MRI. J Xray Sci Technol. 2003;11(4): 231–40. [PubMed: 22388293]
12. Li W, Tutton S, Vu AT, et al. First-pass contrast-enhanced magnetic resonance angiography in humans using ferumoxytol, a novel ultrasmall superparamagnetic iron oxide (USPIO)-based blood pool agent. J Magn Reson Imaging. 2005;21(1):46–52. [PubMed: 15611942]
13. Bashir MR, Bhatti L, Marin D, Nelson RC. Emerging applications for ferumoxytol as a contrast agent in MRI. J Magn Reson Imaging. 2015;41(4):884–98. [PubMed: 24974785]
14. Budjan J, Neudecker S, Schock-Kusch D, et al. Can Ferumoxytol be Used as a Contrast Agent to Differentiate Between Acute and Chronic Inflammatory Kidney Disease?: Feasibility Study in a Rat Model. Invest Radiol. 2016;51(2):100–5. [PubMed: 26352750]
15. Chalouhi N, Jabbour P, Magnotta V, Hasan D. The emerging role of ferumoxytol-enhanced MRI in the management of cerebrovascular lesions. Molecules. 2013;18(8):9670–83. [PubMed: 23945642]
16. Hasan DM, Chalouhi N, Jabbour P, et al. Imaging aspirin effect on macrophages in the wall of human cerebral aneurysms using ferumoxytol-enhanced MRI: preliminary results. J Neuroradiol. 2013;40(3):187–91. [PubMed: 23428244]
17. Ros PR, Freeny PC, Harms SE, et al. Hepatic MR imaging with ferumoxides: a multicenter clinical trial of the safety and efficacy in the detection of focal hepatic lesions. Radiology. 1995;196(2): 481–8. [PubMed: 7617864]
18. Harisinghani M, Ross RW, Guimaraes AR, Weissleder R. Utility of a new bolus-injectable nanoparticle for clinical cancer staging. Neoplasia. 2007;9(12):1160–5. [PubMed: 18084623]
19. Harisinghani MG, Barentsz J, Hahn PF, et al. Noninvasive detection of clinically occult lymph-node metastases in prostate cancer. N Engl J Med. 2003;348(25):2491–9. [PubMed: 12815134]
20. Turkbey B, Agarwal HK, Shih J, et al. A Phase I Dosing Study of Ferumoxytol for MR Lymphography at 3 T in Patients With Prostate Cancer. AJR Am J Roentgenol. 2015;205(1):64–9. [PubMed: 26102381]
21. Corot C, Robert P, Idee JM, Port M. Recent advances in iron oxide nanocrystal technology for medical imaging. Adv Drug Deliv Rev. 2006;58(14):1471–504. [PubMed: 17116343]
22. Wilson GJ, Springer CS, Jr., Bastawrous S, Maki JH. Human whole blood 1 H2 O transverse relaxation with gadolinium-based contrast reagents: Magnetic susceptibility and transmembrane water exchange. Magn Reson Med. 2017;77(5):2015–27. [PubMed: 27297589]
23. Wilson GJ, Woods M, Springer CS, Jr., et al. Human whole-blood (1)H2O longitudinal relaxation with normal and high-relaxivity contrast reagents: influence of trans-cell-membrane water exchange. Magn Reson Med. 2014;72(6):1746–54. [PubMed: 24357240]
24. Hernando D, Kramer JH, Reeder SB. Multipeak fat-corrected complex R2* relaxometry: theory, optimization, and clinical validation. Magn Reson Med. 2013;70(5):1319–31. [PubMed: 23359327]
25. Shen Y, Goerner FL, Snyder C, et al. T1 relaxivities of gadolinium-based magnetic resonance contrast agents in human whole blood at 1.5, 3, and 7 T. Invest Radiol. 2015;50(5):330–8. [PubMed: 25658049]
26. de Bazelaire CM, Duhamel GD, Rofsky NM, Alsop DC. MR imaging relaxation times of abdominal and pelvic tissues measured in vivo at 3.0 T: preliminary results. Radiology. 2004;230(3):652–9. [PubMed: 14990831]
27. Bullivant JP, Zhao S, Willenberg BJ, et al. Materials characterization of Feraheme/ferumoxytol and preliminary evaluation of its potential for magnetic fluid hyperthermia. Int J Mol Sci. 2013;14(9): 17501–10. [PubMed: 24065092]

28. Zhang Y, Poirier-Quinot M, Springer CS, Jr., Balschi JA. Active trans-plasma membrane water cycling in yeast is revealed by NMR. Biophys J. 2011;101(11):2833–42. [PubMed: 22261073]

29. FDA 2015;Pages. Accessed at https://www.fda.gov/safety/medwatch/safetyinformation/safetyalertsforhumanmedicalproducts/ucm440479.htm. Accessed Oct 5, 2017 2017.

30. MHRA 2014;Pages. Accessed at https://www.gov.uk/drug-safety-update/ferumoxytol-risk-of-serious-hypersensitivity-reactions-contraindicated-if-any-drug-allergy-administer-via-infusion. Accessed Oct 5, 2017 2017.

31. Curtis R 2015;Pages. Accessed at https://assets.publishing.service.gov.uk/media/55159aa7ed915d142400005f/Rienso_DHPC_sent_13_March_2015.pdf. Accessed Oct 5, 2017 2017.

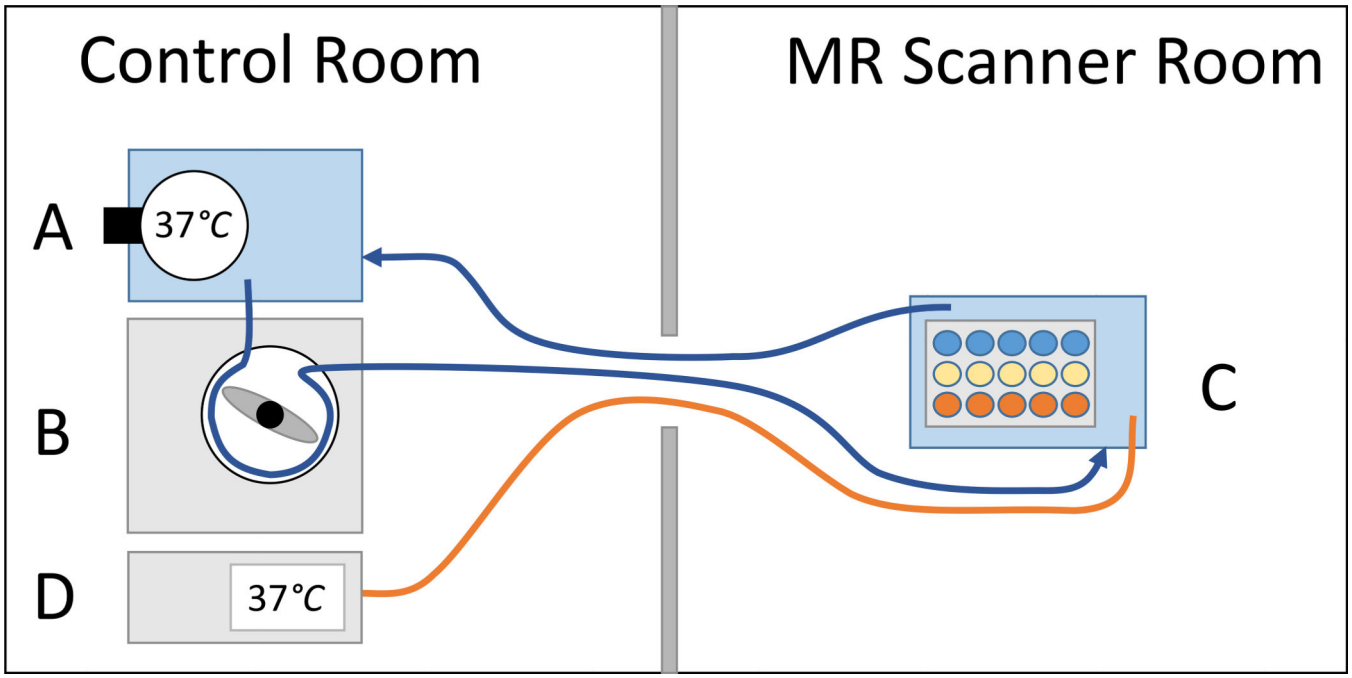

Figure 1:
Setup of circulating water bath. Water was heated to 37°C in a first water bath in the control room using a revolving heater (A). A roller pump (B) was used to pump the heated water into a second water bath inside the MR scanner, which contained the ferumoxytol vials (C), and back into the first water bath. To monitor the actual water temperature inside the MR scanner, an MR compatible thermometer (D) was placed in the MR-control room and the tip of its fiberoptic probe was placed in the phantom-containing water bath inside the MR-scanner.

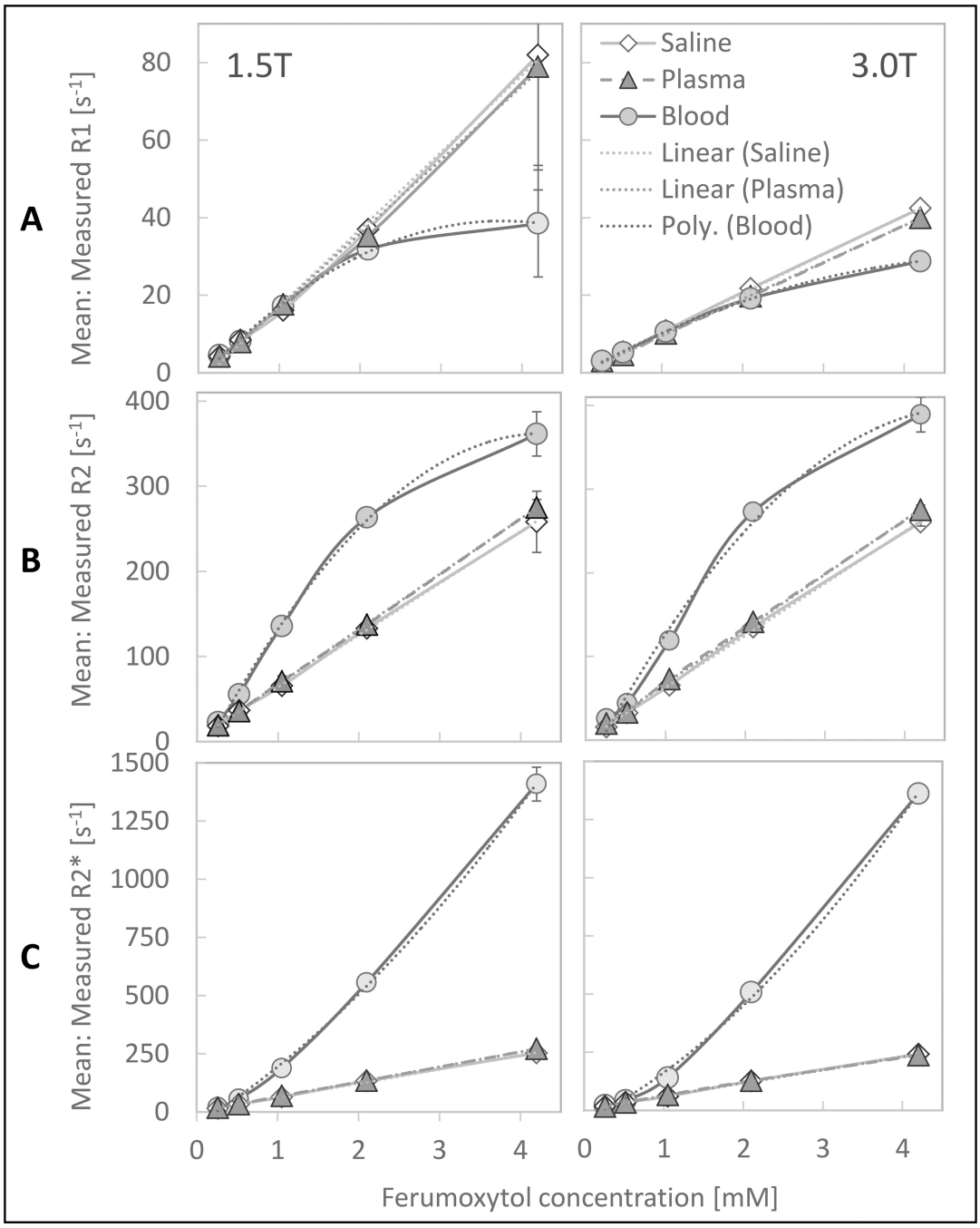

Figure 2:

There is a linear relationship of R1, R2 and R2* in saline and plasma and nonlinear relationship in blood with increasing ferumoxytol concentrations at 1.5T and 3.0T. The plots show (**A**:) the mean measured longitudinal relaxivity rates, R1, (**B**:) mean transverse relaxivity rates, R2, and (**C**:) mean transverse relaxivity rates from free induction decay, R2* with standard deviations (error bars) of different ferumoxytol concentrations in saline, plasma and whole blood at 37°C at 1.5T (left) and 3.0T (right). Note: most error bars are too small to be depicted by the plots.

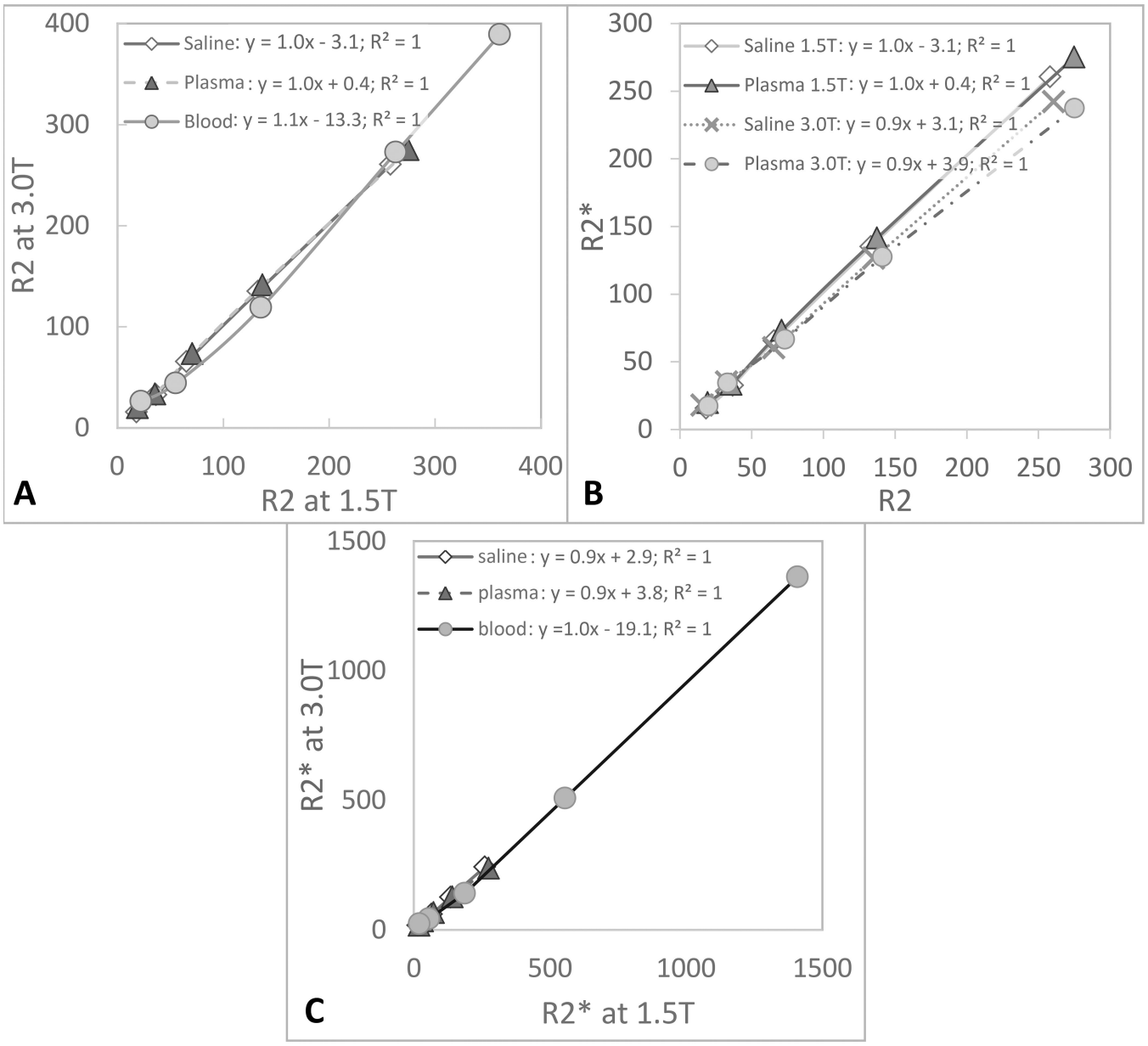

Figure 3A:
The linear dependence with a slop of ~1 illustrates the independence of R2 from the field strength. The plot shows the measured mean R2 values at 1.5T and 3.0T at the six investigated ferumoxytol concentrations in saline, plasma and blood. **3B:** The linear dependence with a slope of close to one illustrates that R2 and R2* values are almost identical at both field strengths with little to no refocusable spins in saline and plasma. The plot shows the measured mean R2 and R2* values at 1.5T and 3.0T at the six investigated ferumoxytol concentrations in saline and plasma. **3C:** The linear dependence with a slop of ~1 illustrates the independence of R2* from the field strength. The plot shows the measured mean R2* values at 1.5T and 3.0T at the six investigated ferumoxytol concentrations in saline, plasma and blood.

Table 1:

Acquisition parameters for R1, R2 and R2* measurement at 1.5T and 3.0T

	R1		R2	R2*			
	1.5T	3.0T	1.5T and 3.0T	1.5T		3.0T	
				High concentrations (1.05 – 4.2 mM)	Low concentrations (0.26 – 0.52 mM)	High concentrations (1.05 – 4.2 mM)	Low concentrations (0.26 – 0.52 mM)
	2D IR-FSE	2D IR-FSE	2D SE	3D spoiled GRE	3D spoiled GRE	3D spoiled GRE	3D spoiled GRE
Inversion time [ms]	50, 57, 65, 75, 119, 188, 300, 488, 669, 1000	50, 57, 65, 75, 119, 188, 300, 488, 669, 1000	n.a.	n.a.	n.a.	n.a.	n.a.
TR [ms]	2500	2500	2000	9.6	14.8	6.1	9.2
TE [ms]	7.69	6.89	6, 7, 8, 9, 10, 11, 12, 15, 17, 20, 23, 26, 31, 41, 47, 55, 64, 74, 86, and 100	0.75, 1.42, 2.09, 2.76, 3.43, 4.1, 4.77, 5.44, 6.11, 6.78, 7.45, 8.12	1.19, 3.16, 5.13, 7.1, 9.07, 11.04	0.66, 1.24, 1.82, 2.4, 2.98, 3.56, 4.14, 4.72	1.43, 2.59, 3.76, 4.92, 6.08, 7.25
Number of echoes	1	1	20	12	6	8	6
Flip angle [degrees]	180, 90	180, 90	90, 180	12	5	9	3
Receiver BW [±kHz]	62.5	62.5	83	125	125	143	125
Acquisition matrix	160 × 160	160 × 160	128 × 128	160 × 128	240 × 160	144 × 128	256 × 256
FOV [mm]	380 × 266	380 × 266	380 × 266	400 × 320	400 × 360	400 × 320	320 × 256
Number of slices	3	3	3	32	32	32	48
Slice thickness [mm]	10	10	10	5	5	5	3
Slice spacing [mm]	18	18	18	n.a.	n.a.	n.a.	n.a.

Table 2:

Measured mean relaxivity values (r1, r2 and r2*) with standard deviations (STD) of ferumoxytol in saline, plasma and blood at 1.5T and 3.0T

			1.5T						3.0T					
	Ferumoxytol concentration		Saline		Plasma		Blood		Saline		Plasma		Blood	
	mM	Vol.	Mean	STD	Mean	STD	Mean	STD	Mean	STD	Mean	STD	Mean	STD
R1 [s^{-1}]	4.2	1/128	82.0	28.5	78.9	31.8	38.5	13.8	42.4	1.3	40.0	2.0	28.8	1.4
	2.1	1/256	37.0	0.9	35.3	0.5	31.8	0.8	21.8	0.2	19.7	0.3	19.2	0.5
	1.1	1/512	16.1	1.1	17.7	0.3	17.2	0.7	11.0	0.0	10.1	0.2	10.6	0.3
	0.5	1/1024	8.4	0.1	7.9	0.1	8.2	0.1	5.4	0.0	4.6	0.1	5.3	0.0
	0.3	1/2048	4.2	0.0	4.2	0.0	4.6	0.0	3.1	0.1	3.0	0.1	3.0	0.1
R2 [s^{-1}]	4.2	1/128	258.2	36.0	275.0	9.5	361.4	26.0	260.6	4.8	275.2	5.6	389.1	20.9
	2.1	1/256	133.1	3.4	137.4	6.2	263.3	9.8	135.2	1.4	141.4	2.1	272.7	4.7
	1.1	1/512	65.6	1.5	71.0	2.1	135.8	2.6	65.5	0.5	73.2	1.1	119.0	2.2
	0.5	1/1024	36.8	1.6	35.8	0.7	55.5	7.3	32.6	0.4	33.3	0.7	44.1	1.0
	0.3	1/2048	18.3	0.7	19.3	1.3	22.7	1.0	15.5	0.5	19.8	0.2	26.0	0.4
R2* [s^{-1}]	4.2	1/128	253.3	9.3	271.3	12.6	1409.0	73.2	242.2	4.4	237.3	7.6	1361.9	28.0
	2.1	1/256	132.7	6.4	134.2	5.8	555.8	24.0	126.4	2.5	127.4	2.6	508.2	9.6
	1.1	1/512	63.5	4.5	68.8	4.9	187.8	7.2	60.3	5.1	66.4	4.1	141.1	4.5
	0.5	1/1024	35.6	3.7	35.5	4.5	64.7	5.3	35.7	5.9	34.4	5.8	44.8	4.2
	0.3	1/2048	16.5	2.5	17.8	3.3	21.4	3.7	17.3	4.0	16.7	4.6	22.6	9.7

Table 3:

Longitudinal relaxivity (r1) and transverse relaxivities (r2 and r2*) including correlation coefficient (r^2) and standard errors (SE) of ferumoxytol measured in saline, human plasma, and human whole blood at 1.5T and 3.0T. Fittings of saline and plasma were linear, therefore their relaxivities (r1, r2, r2*) are represented by the slope of the equation. Fitting of blood was non-linear wherefore relaxivities can only be presented in as a 2nd order polynomial regression.

		Longitudinal relaxivity			Transverse relaxivity					
		r1 (s-1 mM-1)	r^2	SE	r2 (s-1 mM-1)	r^2	SE	r2* (s-1 mM-1)	r^2	SE
Saline	1.5T	y = 19.89× - 2.79	0.997	2.3	y = 60.77× + 3.58	1.000	3.8	y = 60.43× + 1.32	0.999	4.7
	3.0T	y = 10.03× + 0.43	1.000	0.3	y = 62.29× + 0.59	1.000	3.7	y = 57.02× + 3.60	0.999	4.7
Plasma	1.5T	y = 19.01× - 2.10	0.997	1.7	y = 64.85× + 2.25	1.000	1.8	y = 64.41× + 0.31	1.000	2.5
	3.0T	y = 9.46× + 0.09	0.999	0.2	y = 65.17× + 2.62	1.000	1.8	y = 55.66× + 6.03	0.999	4.4
Blood	1.5T	y = −2.89×^{2} + 21.75× - 1.72	0.998	1.1	y = −21.15×^{2} + 181.79× - 28.5	0.999	6.6	y = 31.24×^{2} + 218.06× - 55.39	0.999	27.3
	3.0T	y = −1.067×^{2} + 11.36× - 0.09	1.000	0.3	y = −18.65×^{2} + 179.61× - 34.23	0.993	18.7	y = 39.79×^{2} + 169.12× - 46.51	0.999	38.3